<center>**Supporting Information**</center>

Fast Self-Assembly of Polystyrene-*b*-Poly(fluoro methacrylate) with Sub-5 nm Microdomains for Nanopatterning Applications

Xuemiao Li, Jie Li, Chenxu Wang, Yuyun Liu and Hai Deng*

Department of Macromolecular Science and State Key Laboratory of Molecular Engineering of Polymers, Fudan University, Shanghai 200433 (P. R. China)
E-mail: haideng@fudan.edu.cn

1. Methods

Materials. Styrene (>99% stabilized), *sec*-butyllithium (*sec*-BuLi, 1 M in hexane), dibutylmagnesium (MgBu$_2$,1 M in hexane), dibutylzinc (ZnBu$_2$, 1 M in toluene), 1,1-diphenylethylene (DPE), and calcium hydride (CaH$_2$) powder were purchased from Energy Chemical. Pentadecafluorooctyl methacrylate (PDFMA, 97% stabilized) was purchased from J&K and lithium chloride was bought from Alfa Aesar. All solvents (tetrahydrofuran (THF), methanol) were obtained from Titan.

Reagents Purification. Styrene, THF, and DPE were freshly distilled from CaH$_2$. PDFMA was purified by passing through an alumina column, and then treated with ZnBu$_2$. All other reagents and solvents were used as received unless otherwise noted.

Block Copolymerization of PS-*b*-PPDFMA. Each block copolymer (PS-*b*-PPDFMA) was synthesized according to the following procedure. The flask was dried under vacuum and purged with argon 3 times. 25-35 mL of THF and 1-5 mL of styrene were transferred to a flask loaded with dry LiCl (5 eq. of the initiator). The flask was

cooled to −80 °C - −85 °C, and 0.5 mL of *sec*-butyllithium (1 M in hexane) was injected. After 30 min of polymerization, styryl anions were capped with 0.1 mL of DPE. Then 1.5 mL pentadecafluorooctyl methacrylate monomer was added into the system and polymerized for 30 min, and then terminated with 0.5 mL of degassed methanol. The solution was precipitated with methanol twice and the resulting white powder was dried in vacuum.

Characterization. Nuclear magnetic resonance (NMR, ^{1}H, 400MHz; ^{19}F, 376 MHz) spectra were acquired on a Varian MERCURY 400 NMR spectrometer at 298 K using CDCl$_3$ as a solvent and tetramethylsilane (TMS) as an internal standard. Gel permeation chromatography (GPC) was carried out on a Shimadzu Prominence LC-20A, using two Shimadzu KF columns operating at 30 °C. Prominence SPD-20A UV-VIS (254 nm wavelength) and Prominence RID-20A refractive index detectors were operated together (THF as eluent). Gas Chromatography (GC) analyses were carried out on a Shimadzu GC-2014C to monitor the conversion rate. Differential scanning calorimetry (DSC) was performed on a TA Instruments Q2000. Measurements were taken within the temperature ranging from -50 °C to 160 °C as a rate of 10 °C/min upon the second heating. Small-angle X-ray scattering (SAXS) patterns were collected on a Nanostar SAXS (Bruker AXS GmbH, Germany), with pinhole collimation for point focus geometry. The X-ray source was a copper sealed target operating at 50 kV and 600 μA, fitted with cross-coupled Göbel mirrors, resulting in a Cu Kα radiation wavelength of 1.54 Å. The SAXS instrument was equipped with a Vantec-2000 2D detector. The distance between the sample and detector was calibrated using silver behenate, giving

the scattering vector q a range from 0.07 to 2.3 nm^{-1}, where q is the magnitude of the scattering vector defined as q = 4πsinθ/λ, λ is the wavelength, and 2θ is the scattering angle. The optics and sample chamber were under vacuum to minimize air scatter. The SAXS profiles were normalized to sample transmission, the background was subtracted, and then the profiles were radially averaged using the SAXSNT software package (Bruker AXS GmbH, Germany).

For transmission electron microscopy (TEM) measurements, bulk samples were prepared on copper TEM grids. Brightfield (BF-TEM) images were taken with a FEI Tecnai G2 20 TWIN electron microscope equipped with a FEI BM-eagle CCD camera, operated at an acceleration voltage of 200 kV. Field emission scanning electron microscope (FESEM) images were observed with a Zeiss Ultra 55 with In-lens detector at 3 kV. Atomic force microscopy (AFM) images of the directed self-assembly pattern in Si templates were measured by Brucker Dimension Fast Scan in Peak Force mode. Rheology tests were performed on an Thermofisher HAAKE MARS III rheometer at a temperature rate of 1 °C/min.

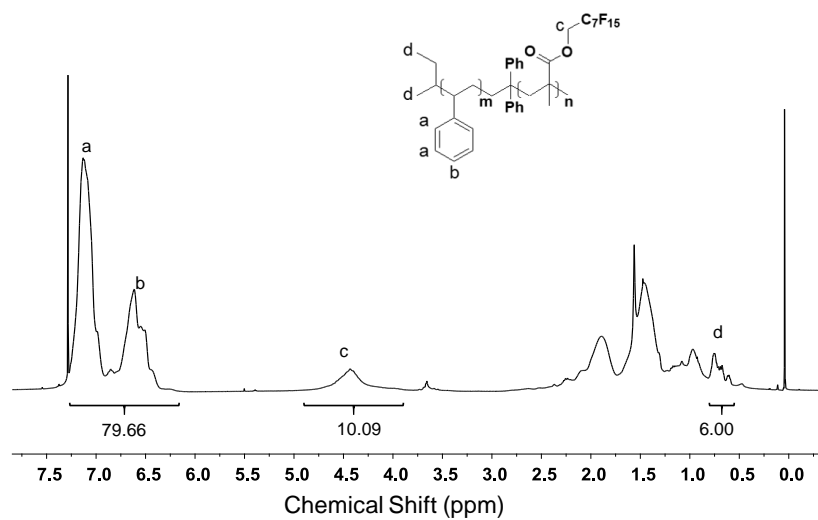## 2. Characterization of PS-*b*-PPDFMA

### 2.1 ^{1}H NMR and ^{19}F NMR spectra of PS-*b*-PPDFMA (polymer S1-S7)
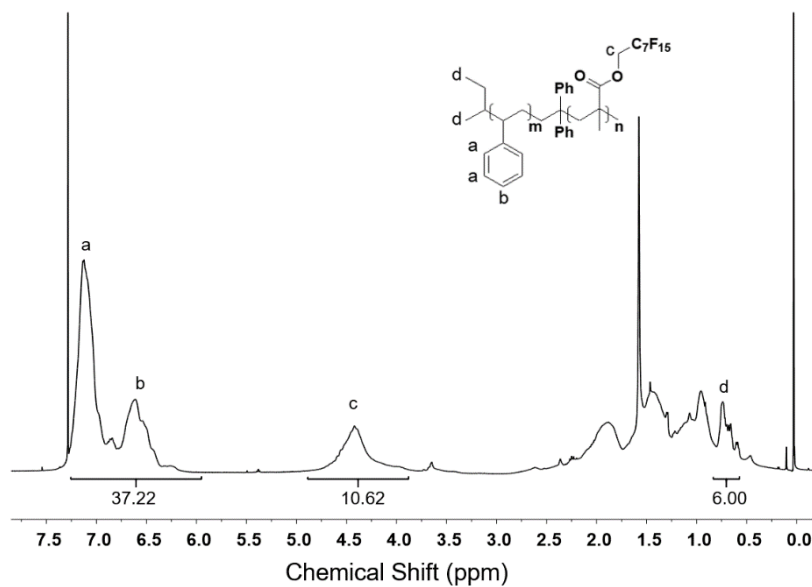
Fig. S1 ^{1}H NMR spectrum of polymer S1 in CDCl$_3$. ^{1}H NMR (400 MHz, CDCl$_3$) δ: 7.24 - 6.23 (5H, Ar-H), 4.42 (2H, OCH$_2$C$_7$F$_{15}$), 0.74 - 0.59 (6H, CH$_3$ of *sec*-Bu).
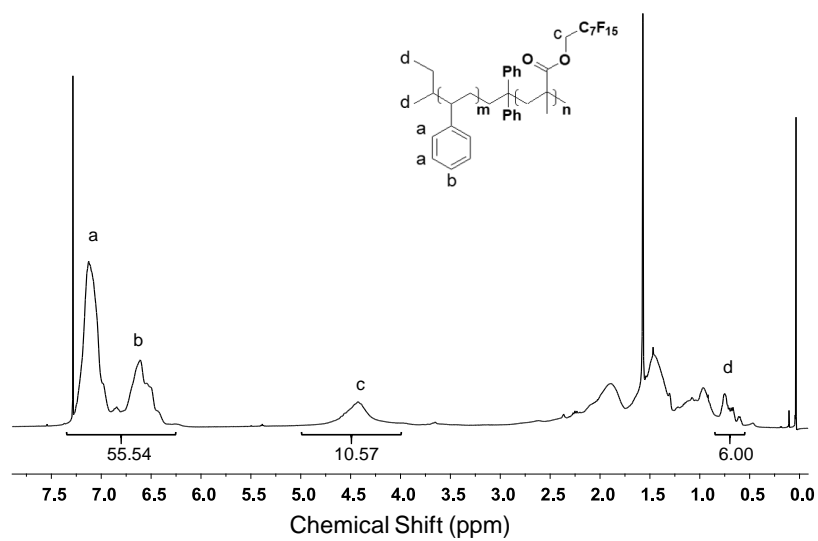
Fig. S2 ^{1}H NMR spectrum of polymer S2 in CDCl$_3$. ^{1}H NMR (400 MHz, CDCl$_3$) δ: 7.24 - 6.26 (5H, Ar H), 4.42 (2H, OCH$_2$C$_7$F$_{15}$), 0.75 - 0.60 (6H, CH$_3$ of *sec*-Bu).

Fig. S3 ^{1}H NMR spectrum of polymer S3 in CDCl$_3$. ^{1}H NMR (400 MHz, CDCl$_3$) δ: 7.24 - 6.26 (5H, Ar H), 4.42 (2H, OCH$_2$C$_7$F$_{15}$), 0.75 - 0.60 (6H, CH$_3$ of *sec*-Bu).
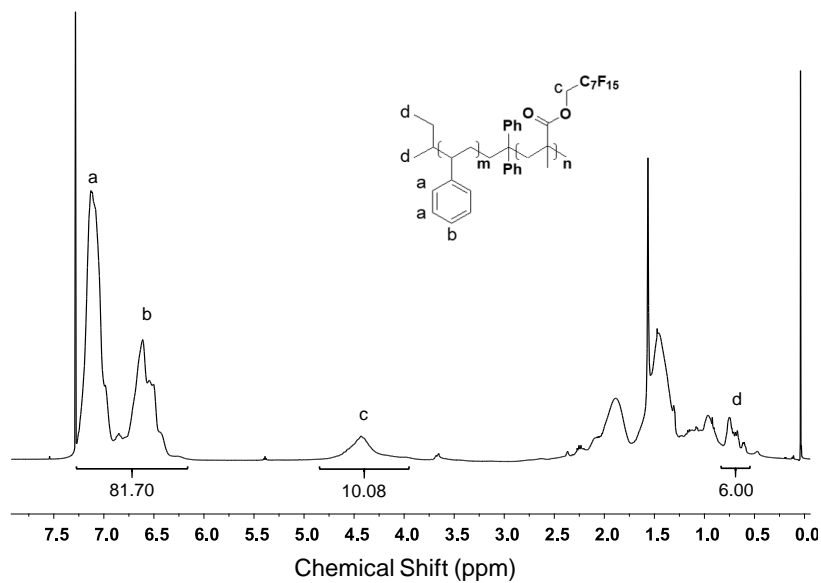
Fig. S4 ^{1}H NMR spectrum of polymer S4 in CDCl3. ^{1}H NMR (400 MHz, CDCl3) δ: 7.25 - 6.24 (5H, Ar-H), 4.43 (2H, OCH$_2$C$_7$F$_{15}$), 0.75 - 0.61 (6H, CH$_3$ of *sec*-Bu).
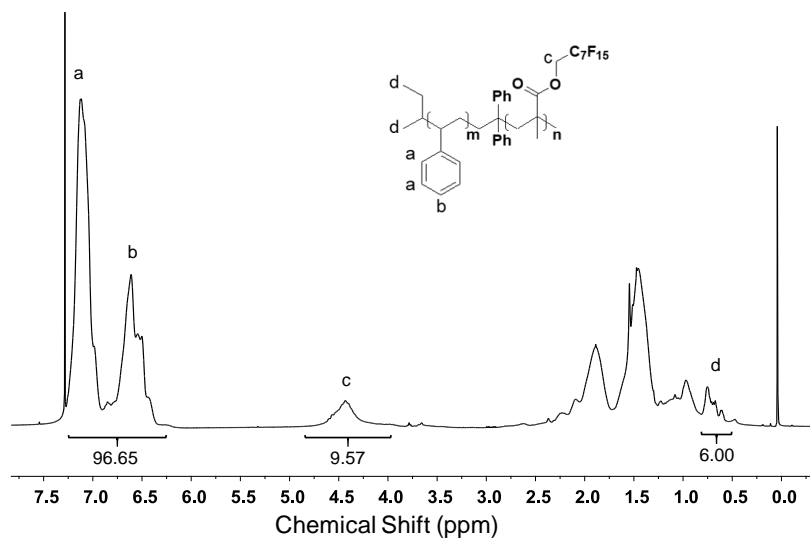
Fig. S5 ^{1}H NMR spectrum of polymer S5 in CDCl3. ^{1}H NMR (400 MHz, CDCl3) δ: 7.24 - 6.26 (5H, Ar H), 4.43 (2H, OCH$_2$C$_7$F$_{15}$), 0.75 - 0.60 (6H, CH$_3$ of *sec*-Bu).
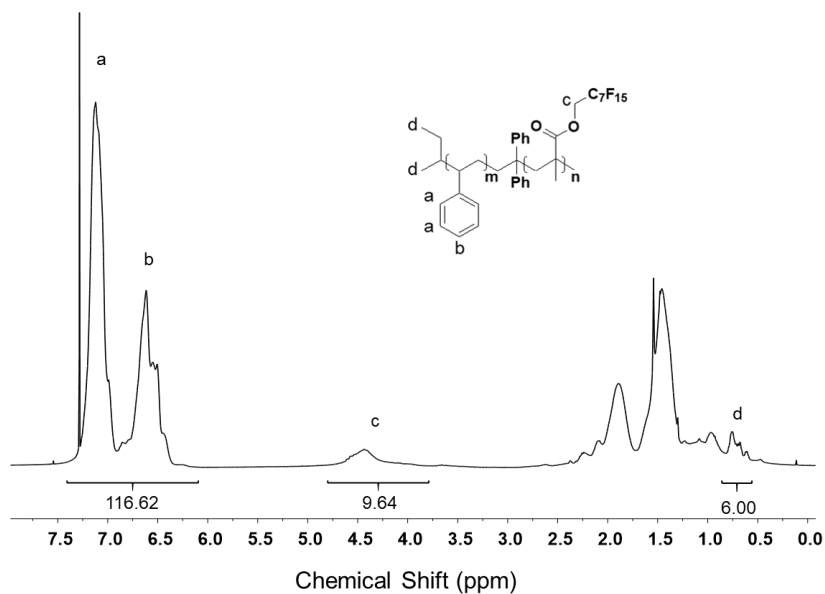
Fig. S6 ^{1}H NMR spectrum of polymer S6 in CDCl₃. ^{1}H NMR (400 MHz, CDCl₃) δ: 7.25 - 6.25 (5H, Ar-H), 4.43 (2H, OCH$_2$C$_7$F$_{15}$), 0.75 - 0.59 (6H, CH$_3$ of *sec*-Bu).
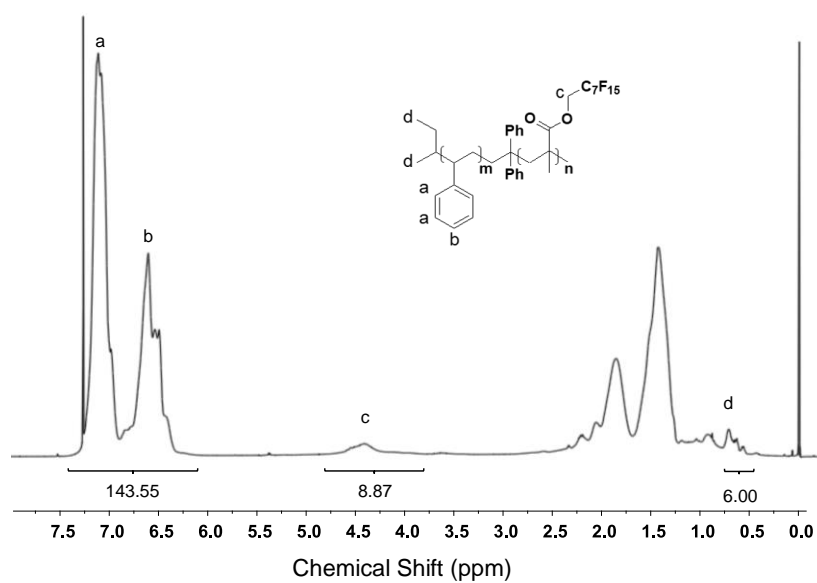
Fig. S7 ^{1}H NMR spectrum of polymer S7 in CDCl₃. ^{1}H NMR (400 MHz, CDCl₃) δ: 7.25 - 6.24 (5H, Ar-H), 4.37 (2H, OCH$_2$C$_7$F$_{15}$), 0.75 - 0.57 (6H, CH$_3$ of *sec*-Bu).
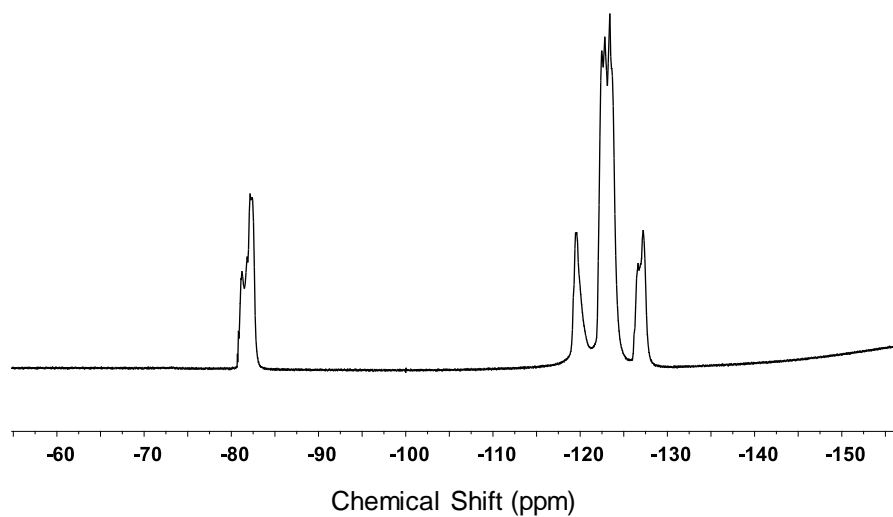
Fig. S8 ^{19}F NMR spectrum of polymer S1 in CDCl$_3$. ^{19}F NMR (376 MHz, CDCl$_3$) δ: -81.3 – -82.2 (3F, CF$_3$), -119.5 – -127.2 (12F, C$_6$F$_{12}$)

2.2 GPC results of block copolymers S1-S7
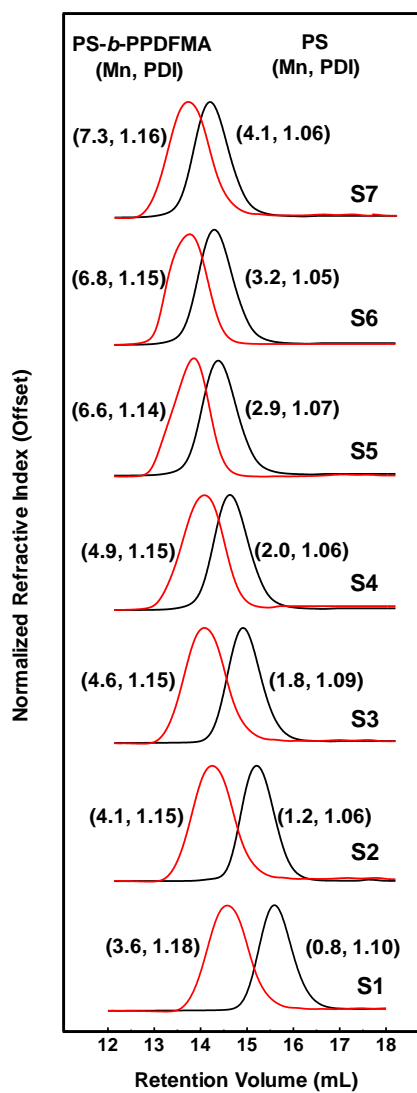
Fig. S9 Overlaid GPC traces of PS homopolymers (black lines) and PS-*b*-PPDFMA block copolymers (red lines) of block copolymers S1-S7.

Table S1. Summary of GPC results of obtained BCPs

| Polymer	M_n [kg mol^{-1}]	PDI
S1	3.6	1.18
S2	4.1	1.15
S3	4.6	1.15
S4	4.9	1.15
S5	6.6	1.14
S6	6.8	1.15
S7	7.3	1.16

Because the PDI of the homopolymers and the resulting copolymers were very narrow and there was no tailing in the GPC curves of the copolymers, we concluded that the resulting copolymers were uniform PS-*b*-PPDFMA block copolymers.

## 2.3 Monitoring of the conversion ratio of monomers in BCPs

In order to verify that all of the styrene monomers were polymerized before the PDFMA monomer was added, we monitored the conversion ratio of styrene monomer after 10 min and 30 min of polymerization. The disappearance of the styrene peak in the GC curves at 10 min indicated that all of the styrene monomers had reacted (Figu S10a). GPC and ^{1}H NMR results (Fig. S11-S13), further illustrated this result. The molecular weight and polydispersity index (PDI) after 10 min and 30 min polymerization were the same (Table S2). Therefore, 30 min of reaction time was adequate for the first block to polymerize as designed. The conversion rate of the fluoro monomers was > 99%, confirmed by GC after methanol quenching (Fig. S10b).
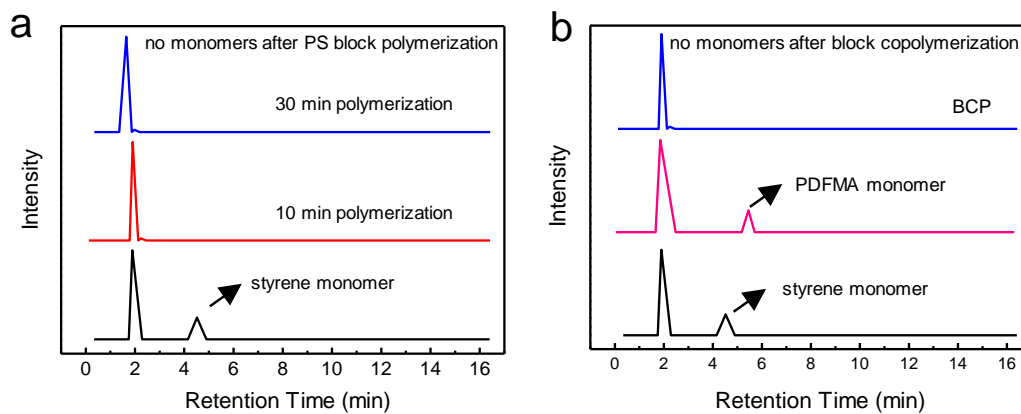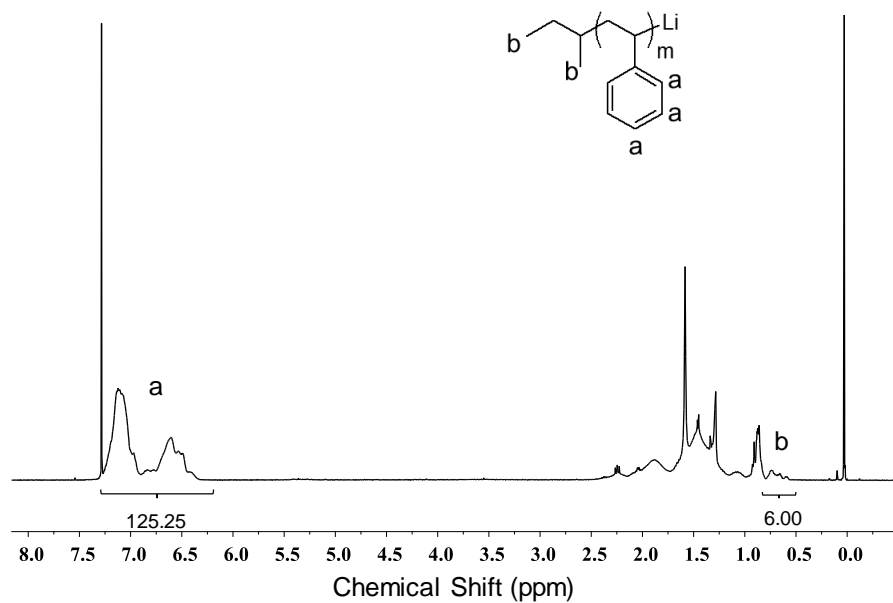
Fig. S10 a) Monitoring of the conversion ratio of styrene by GC. The extent of conversion of styrene was > 99%; b) The extent of conversion of the flouro monomers was > 99%, as confirmed by GC after methanol quench.
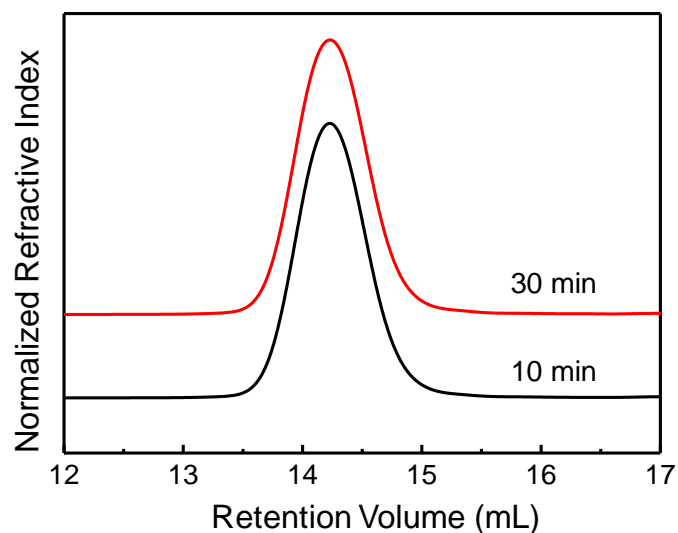
Fig. S11 Overlaid GPC traces of the PS block after 10 min and 30 min of anionic polymerization.
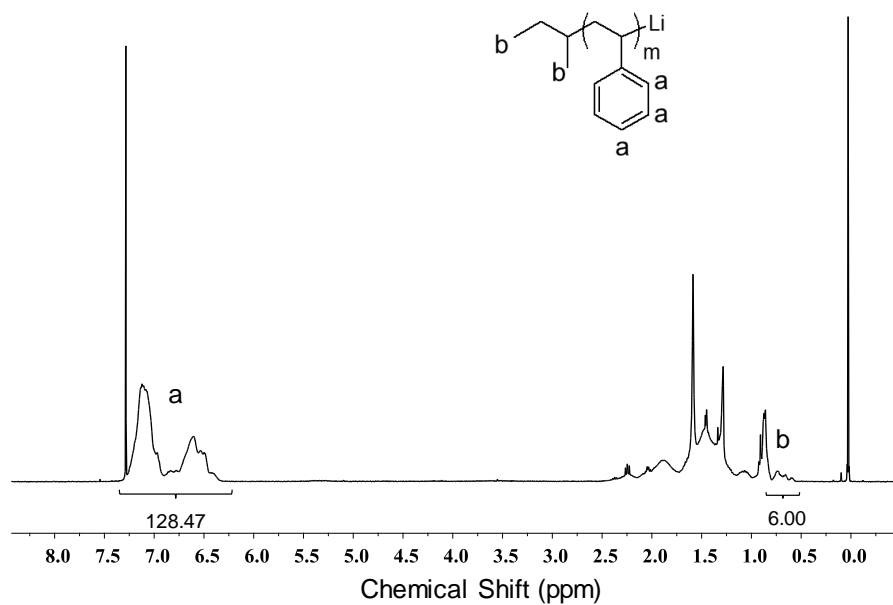
Fig. S12 ^{1}H NMR spectrum of the PS block after 10 min polymerization.

Fig. S13 ^{1}H NMR spectrum of the PS block after 30 min polymerization.

Table S2. GPC results of PS after 10 min and 30 min anionic polymerization

Time	M_n [kg mol^{-1}]	PDI
10 min	3.2	1.05
30 min	3.2	1.05

2.4 DSC curves of obtained BCPs
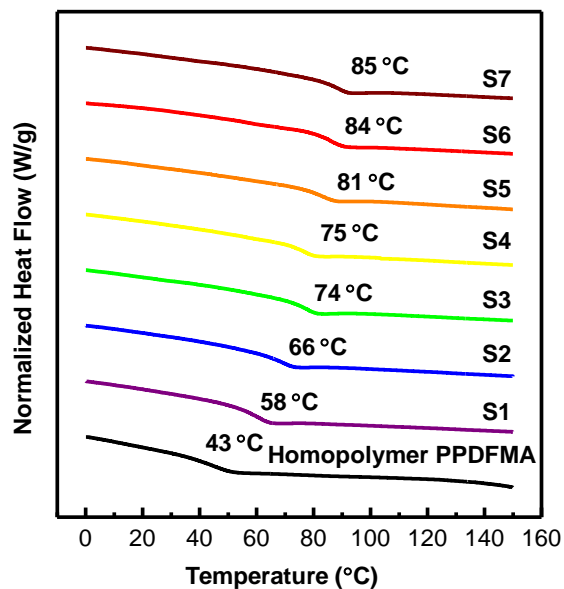
Fig. S14 DSC thermograms for block copolymers S1-S7 and PPDFMA homopolymer are labeled in the diagram. Each thermal scan was taken at a rate of 10 °C/min upon a second heating. The T_g of the individual blocks overlap. The T_g of homopolymer PPDFMA is 43 °C, and T_g values of the PS-*b*-PPDFMAs increased from 58 °C to 85 °C along with the DP of PS block.

2.5 Thermal annealing process
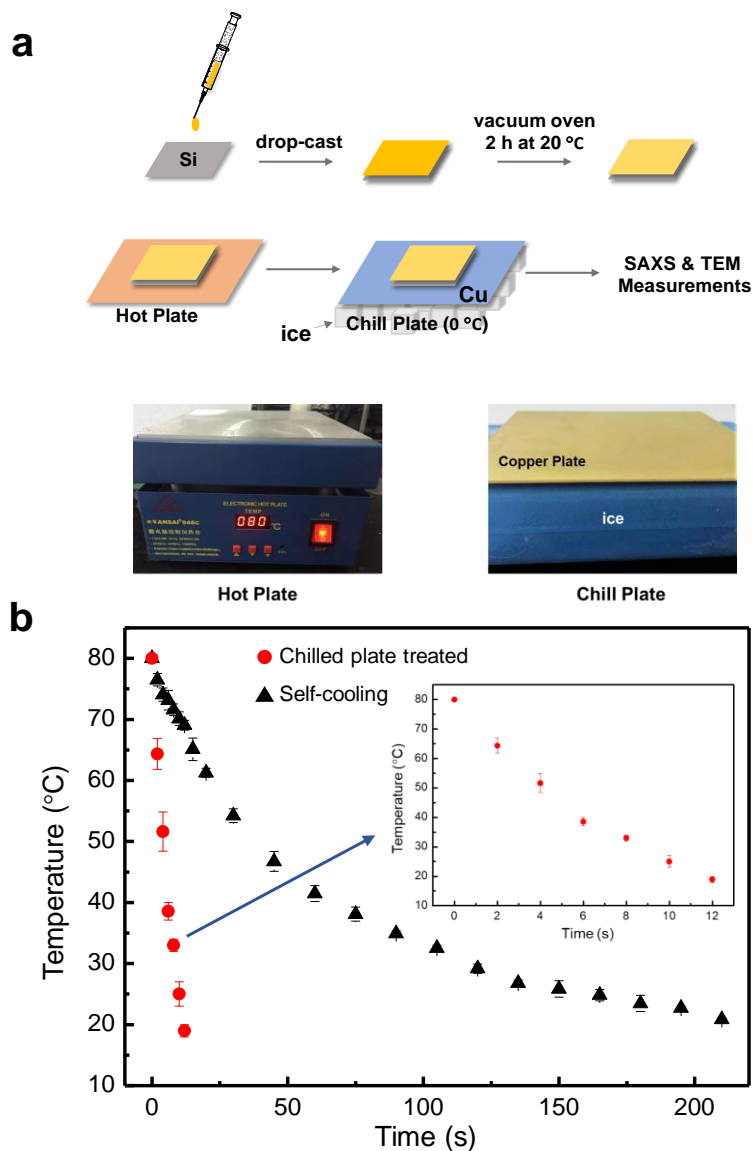
Fig. S15 a) Schematic diagram of the block copolymer (BCP) sample preparation and thermal annealing process, including pictures of the hot plate and the chill plate. For the sample preparation for TEM & SAXS measurements, a 5 wt% BCP solution (in toluene) was drop-cast on the silicon wafer and then dried in vacuum oven at room temperature for 2 h. The film thickness of the thermal annealing sample was nearly 30 μm measured by a super-resolution digital microscope (Keyence, VHX-1000C). The resulting samples were annealed on an 80 °C hot plate, usually for 1 min, and then quenched on a chill plate at 0 °C. b) The cooling curves of samples by self-cooling process (triangle) and fast-chilled process (circle).

3. Calculation of χ-parameter of PS-*b*-PPDFMA via SAXS Analysis

Equations used to fit the disordered state scattering of a block copolymer are shown below.[1,2]

$$I(q) = K[S(q)/W(q) - 2\chi]^{-1}$$

$$S(q) = \; < S_{S,S}(q) > + 2 < S_{S,PDFMA}(q) > + < S_{PDFMA,PDFMA}(q) >$$

$$W(q) = \; < S_{S,S}(q) > * < S_{PDFMA,PDFMA}(q) > - < S_{S,PDFMA}(q) >^2$$

$$< S_{X,X}(q) > \; = r_c f_x^2 g^{(2)}_x(q)$$

$$< S_{S,PDFMA}(q) > \; = r_c f_S f_{PDFMA} g^{(1)}_S(q) \, g^{(1)}_{PDFMA}(q)$$

$$r_c = (v_S N_S + v_{PDFMA} N_{PDFMA}) / (v_S * v_{PDFMA})^{1/2}$$

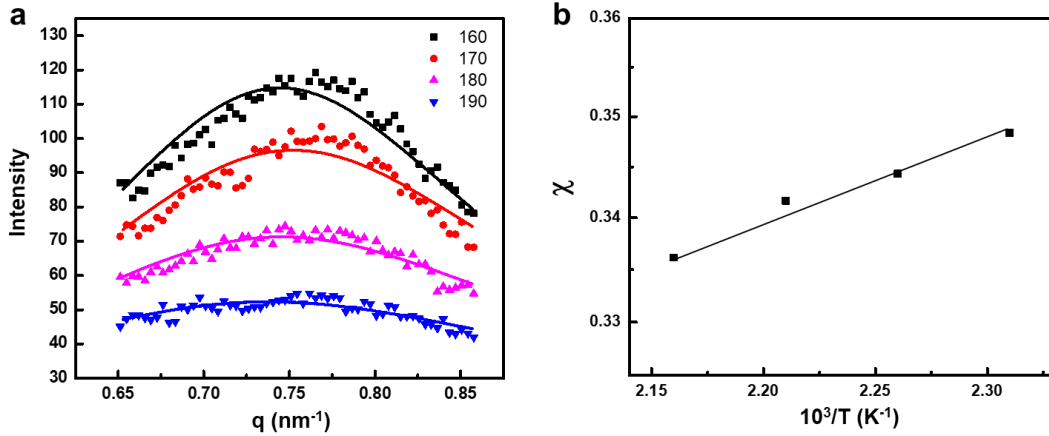$$g^{(1)}_x(q) = 1/ y_x(q) \, \{1 - [y_x(q)(Đ_x - 1) + 1]^{-(Đx-1)-1}\}$$

$$g^{(2)}_x(q) = 2/ y_x(q)^2 \, \{-1 + y_x(q) + [y_x(q)(Đ_x - 1) + 1]^{-(Đx-1)-1}\}$$

$$y_x(q) = (N_x b_x^2/6)q^2$$

$$Đ_s = N_{S,w} / N_{S,n}$$

$$Đ_{PDFMA} = Đ_{BCP} - 1 - (Đ_s - 1)w_s^2/(1 - w_s)^2 + 1$$

Fig. S16 a) SAXS data and fitlines for disordered polymer S8 ($N = 21$) at various temperatures. The best-fit lines were obtained by changing χ as one of the adjustable parameters using Leibler's mean-field theory. Four parameters, including the statistical segment lengths of both polymers and fitting constants K and χ, were optimized to fit the SAXS pattern at a certain temperature. b) Temperature dependence of χ between PS and PPDFMA and the corresponding best fitline. The symmetric, disordered polymer S8 ($N = 21$, $M_n = 2300$, PDI = 1.12) was synthesized

by anionic polymerization as mentioned above.

Table S3. Fitting values for $\chi_{S/PDFMA}$ at the corresponding temperatures

Temperature (°C)	χ (T)
160	0.3484
170	0.3443
180	0.3417
190	0.3362

Temperature dependence of $\chi_{S/PDFMA}$ is expressed by $\chi = 78.51/T + 0.167$

4. T$_{ODT}$ of PS-*b*-PPDFMA BCPs.
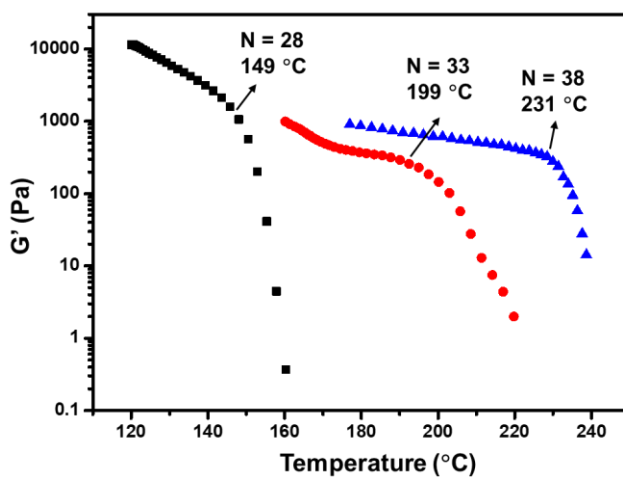
Fig. S17 Temperature dependence of the dynamic storage modulus (G') for S1, S2, and S3. Each sample was taken at strain = 3% and ω = 1 rad/s. The T$_{ODT}$ values were 149 °C, 199 °C, and 231 °C for S1, S2, and S3, respectively.

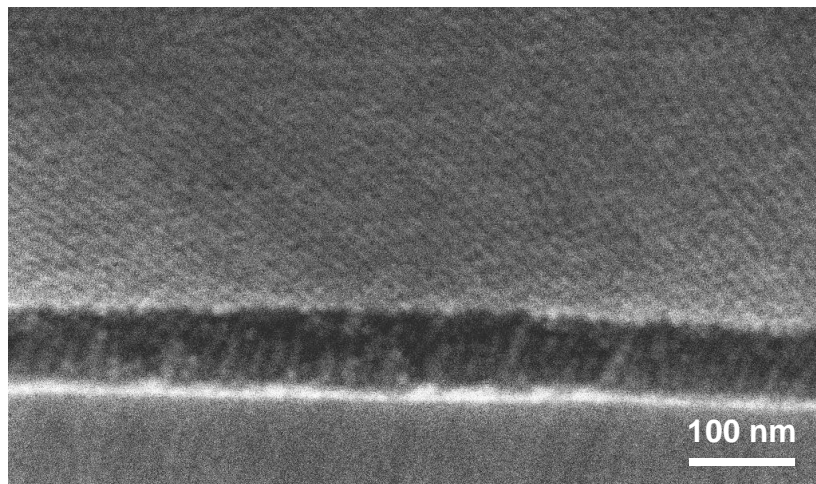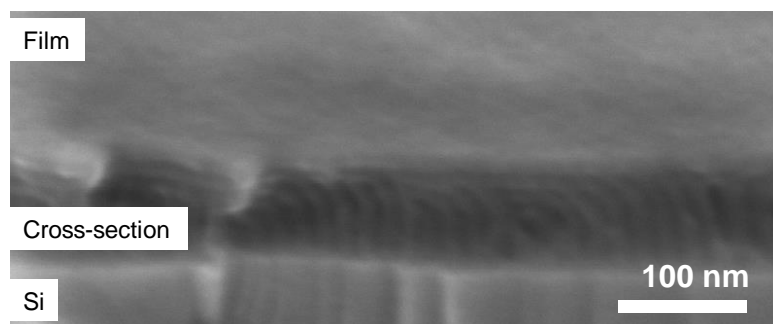## 5. Cross-section SEM images of BCP thin films.

Fig. S18 SEM image (45° tilted) of block copolymer S1.

Fig. S19 45° tilted cross-sectional SEM image of of block copolymer S6 thin film after thermal annealing at 80° C for 1 min.

6. Surface energy measurement of PS and PPDFMA

We measured the surface energy of PS and PPDFMA using the Fowkes equation, shown below. The water and CH_2Cl_2 contact angles were measured at room temperature for each homopolymer film.

$$\gamma_L(1+\cos\theta) = 2(\sqrt{\gamma_L^d \gamma_S^d} + \sqrt{\gamma_L^p \gamma_S^p})$$

Table S4. Contact angle measurement and surface energy calculation of PS and PPDFMA homopolymers.

|	Contact angle H$_2$O (°)	Contact angle CH$_2$I$_2$ (°)	γ (mN m^{-1})
PS	106.9	53.8	40.6
PPDFMA	120.4	98.6	9.7

The surface energy of PS and PPDFMA are 40.6 mN m^{-1} and 9.7 mN m^{-1}, respectively.

7. Synthesis and self-assembly properties of polystyrene-*block*-polydimethylsiloxane (PS-*b*-PDMS) BCPs.

PS-*b*-PDMS BCPs were synthesized by living anionic polymerization as reported.[3] The molecular weight and molar ratio of the two blocks were similar to the blocks of the PS-*b*-PPDFMA BCPs. ^{1}H NMR (400 MHz, CDCl$_3$) δ: 7.26 - 5.80 (5H, Ar-H), 0 - 0.25 (6H, SiO(CH$_3$)$_2$) 0.75 - 0.55 (6H, CH$_3$ of *sec*-Bu).

Table S5. Characterizations of obtained PS-*b*-PDMS BCPs

Block Copolymer	M_n [kg mol^{-1}]	*m/n*	PDI	Full-pitch (Morphology)
PS-*b*-PDMS-1	5400	0.3	1.08	8.7 nm (Lam)
PS-*b*-PDMS-2	5200	1.2	1.11	10.8 nm (Lam)
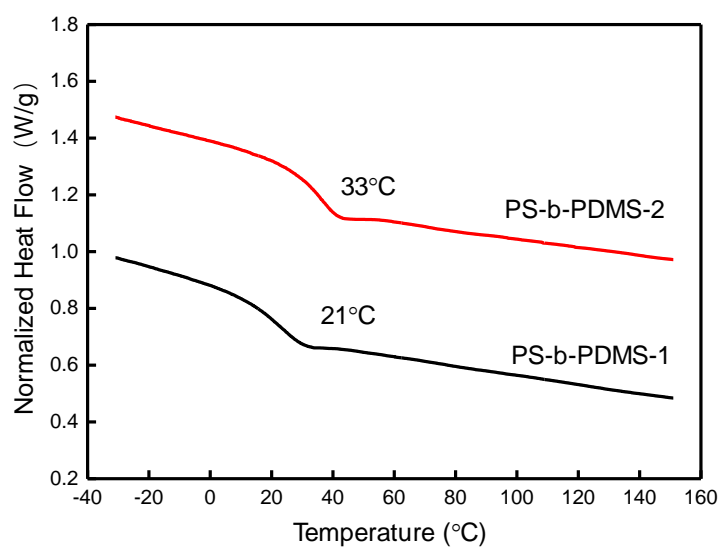
Fig. S20 DSC thermograms for the BCPs PS-*b*-PDMS-1 and PS-*b*-PDMS-2. Each thermal scan was taken at a rate of 10 °C/min upon a second heating. The T_g of the individual blocks overlap.
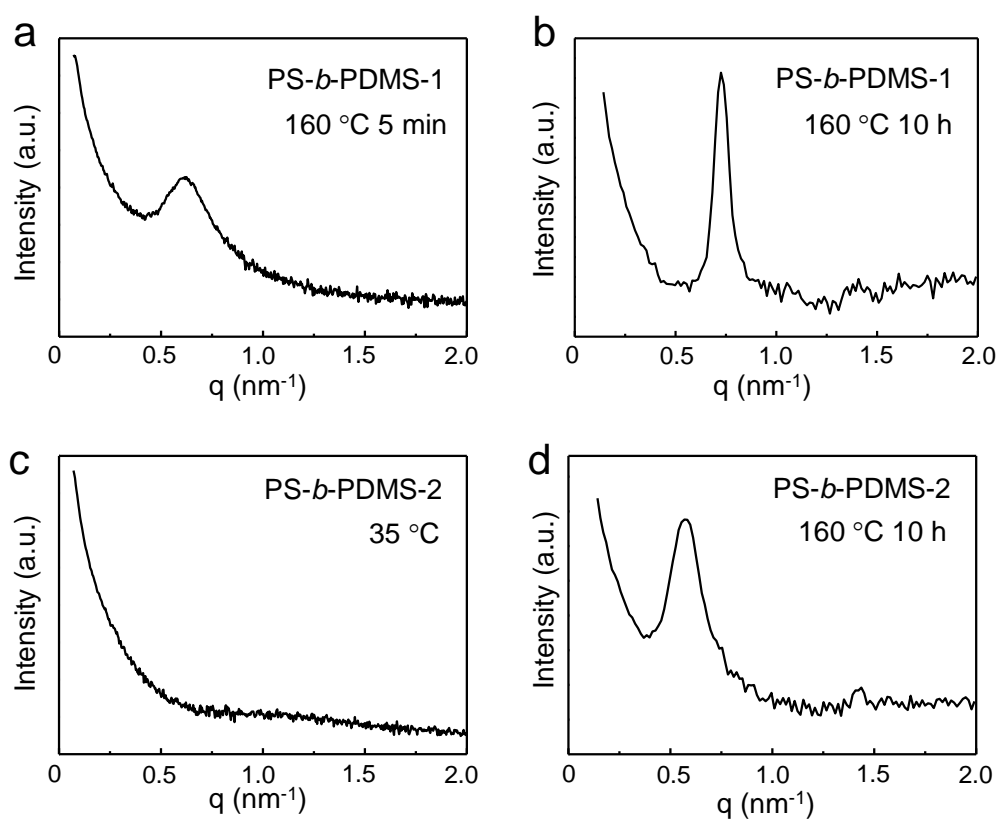
Fig. S21 SAXS 1-D patterns for PS-*b*-PDMS-1 (a) thermally annealed at 160 °C for 5 min, and (b) at 160 °C for 10 h. PS-*b*-PDMS-1 showed a well-defined, sub-10 nm

lamella morphology after annealing at 160 °C for 10 h, however, it did not show any potential for fast annealing. (c) SAXS pattern of PS-*b*-PDMS-2 showed no microphase separation after annealing for several days at 35 °C (above its T_g of 33 °C). (d) PS-*b*-PDMS-2 show lamella morphology after thermal annealing at 160 °C for 10 h.

8. Synthesis and self-assembly properties of polystyrene-*block*-poly(heptafluorobutyl methacrylate) (PS-*b*-PHFBMA) BCPs.
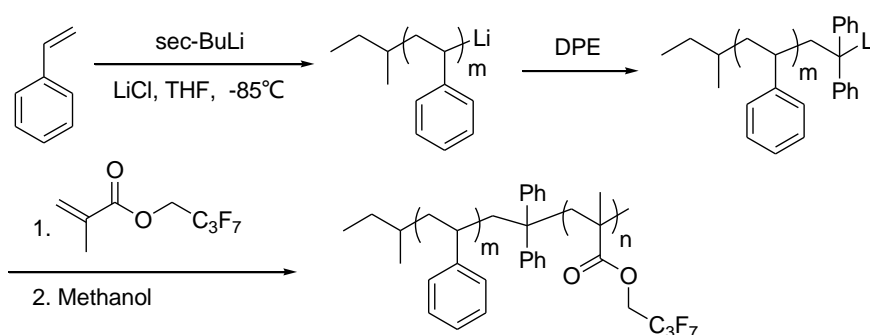

**Scheme S1.** Synthetic route of PS-*b*-PHFBMA.

Anionic copolymerization of PS-*b*-PHFBMA was performed according to the following general procedure. A glass reactor was dried under high vacuum and purged with argon gas 3 times. 25-35 mL of purified THF and 1.5-2.5 mL of freshly distilled styrene were transferred to a glass reactor containing dry LiCl (5 eq of the initiator). The glass reactor was cooled to −80 - −85 °C, and 0.5 mL of *sec*-butyllithium (1 M in cyclohexane) was injected. After 30 min of polymerization, styryl anions were capped with 0.1 mL of DPE. Then 1.5-2 mL heptafluorobutyl methacrylate monomer (purchased from J&K, distilled from AlBu$_3$ before use) was added into the system after 15 min. The reaction was stirred for an additional 30 min and terminated with 0.5 mL of degassed methanol. The solution was precipitated into methanol twice and the resulting white powder was dried in vacuum at elevated temperature.

The obtained PS-*b*-PHFBMA BCPs were characterized by ^{1}H NMR, ^{19}F NMR, and SEC to demonstrate the successful polymerization and determine the molar ratio of the two blocks. ^{1}H NMR (400 MHz, CDCl$_3$, δ): 7.25 - 6.26 (5H; Ar-H), 4.71-4.32 (2H; OCH$_2$C$_3$F$_7$), 0.80 - 0.55 (6H; CH$_3$ of *sec*-Bu).^{19}F NMR (376 MHz, CDCl$_3$, δ): -

80.9 – -82.1 (3F; CF$_3$), -119.7 – -121.3 (2F; -CH$_2$-CF$_2$-), -127.0 – -128.5 (2F; -CF$_2$-CF$_3$). The degree of polymerization of each block is represented by m and n values, which were calculated by the integration values of the arene hydrogens in the styrene and the ethyl in the PHFMBA block divided by the integration values of the *sec*-BuLi methyl end-group, respectively, based on one sec-butyl group per chain in the living anionic polymerization. A summary of the results for each PS-*b*-PHFBMA BCP is given in Table S6.

Table S6. Characterization of obtained PS-*b*-PHFBMA BCPs

Polymer	M_n [kg mol^{-1}]	m	n
PS-*b*-PHFBMA-1 **(H1)**	2.3	8.4	4.9
PS-*b*-PHFBMA-2 **(H2)**	3.3	18.8	4.6
PS-*b*-PHFBMA-3 **(H3)**	4.1	14.2	9.2
PS-*b*-PHFBMA-4 **(H4)**	4.9	17.5	11.1
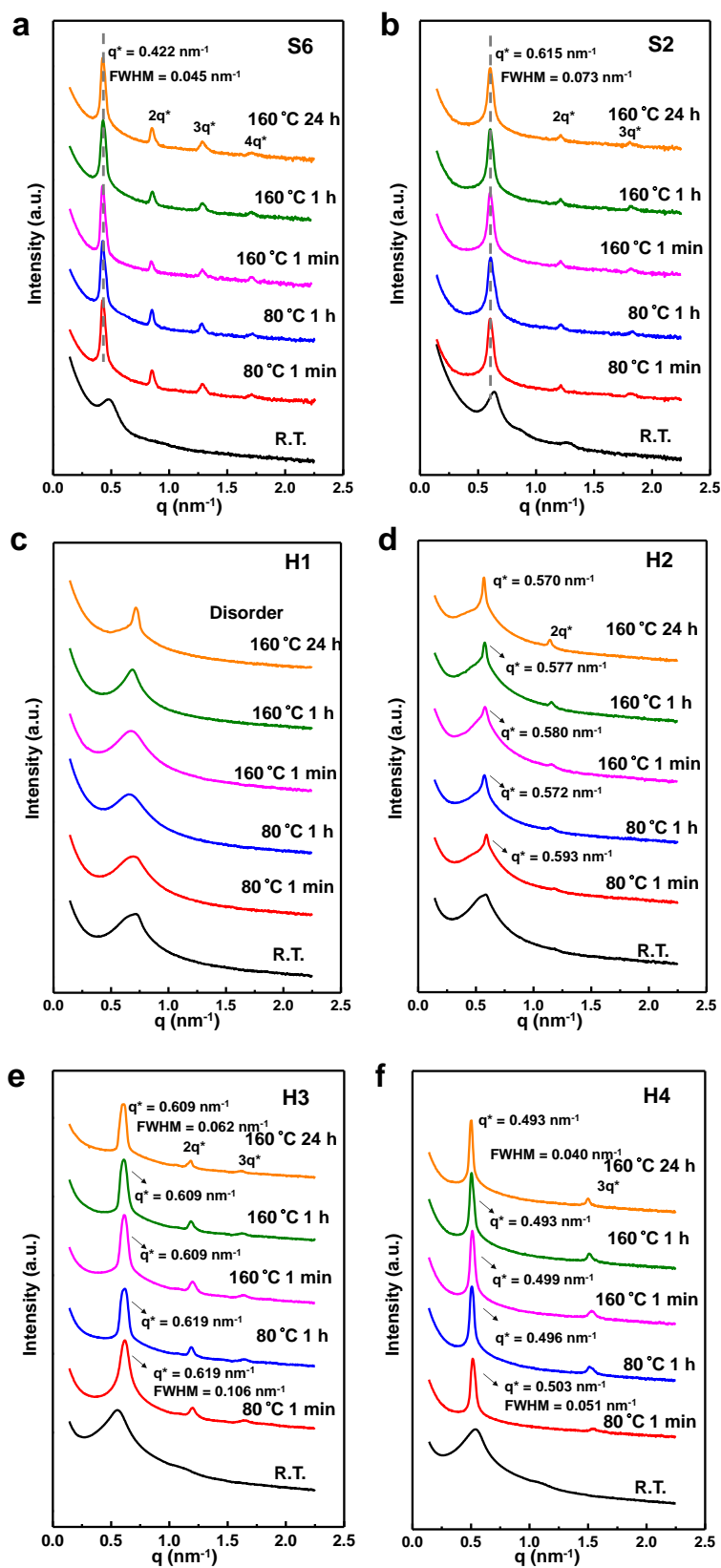
Fig. S22 SAXS 1-D patterns for S2, S6, H1, H2, H3 and H4, after thermal annealing at 80 °C for 1 min and 1 h, and at 160 °C for 1 min, 1 h, and 24 h.

Table S7. The block lengths (*m* and *n*) of block copolymers (BCPs) S2, S6, and H1-4.

BCP	*m*	*n*
S2 ($-CH_2C_7F_{15}$)	9.1	5.3
S6 ($-CH_2C_7F_{15}$)	21.3	4.8
H1 ($-CH_2C_3F_7$)	8.4	4.9
H2 ($-CH_2C_3F_7$)	18.8	4.6
H3 ($-CH_2C_3F_7$)	14.2	9.2
H4 ($-CH_2C_3F_7$)	17.5	11.1

With BCPs H1-H4 we could compare their assembly to the corresponding BCPs S2 and S6, and determine the effect of the reduced F content in the PHFBMA block, relative to the PPDFMA block, on the assembly of the BCPs. A comparison of the their *m* and *n* values is shown in Table S7, and the results of SAXS analysis after annealing of the BCPs is shown in Fig. S22. From this analysis, three main points can be concluded.

1. For the same *n* value, the BCP having more fluorine in the side chain unit is more likely to microphase separate, and will self-assembly more quickly. We compared the self-assembly behavior of BCPs S6 and S2 with BCPs H1 and H2 (Fig. S22a-d). These 4 BCPs had the same value of *n*, the DP of the fluoroalkyl block ($-CH_2C_7F_{15}$ or $-CH_2C_3F_7$), which was ~5. H1 did not show long-range order after thermal annealing, while S2 self-assembled very quickly with 10.2 nm domain spacing. Note that S2 and H1 have the same *m* and *n*.

BCP H2 microphase separated to an ordered structure, but the position of the first peak in SAXS (q*) shifted when the annealing conditions changed. In comparison, BCP S6 self-assembled very quickly, and q* stayed constant at 0.422 nm^{-1} with the same peak sharpness and same FWHM (peak width at half height) of 0.045 nm^{-1}.

2. For the same M_w of the fluorinated block, the BCP having more fluorine in the side chain unit is more likely to microphase separate, and will self-assembly more

quickly. Because of the difference in molecular weight of the monomers containing the perfluoroalkyl ($-CH_2C_7F_{15}$) and heptafluoroalkyl ($-CH_2C_3F_7$) side chains, which were 468 kg mol^{-1} and 268 kg mol^{-1}, respectively, we could examine assembly of two BCPs that had the same M_n but different n of the fluoro blocks (S6 and H3, 468 * 4.8 ≈ 268 * 9.2). Upon annealing, q* value of H3 changed a little when the annealing condition changed, but the FWHM changed significantly, from 0.106 nm^{-1} to 0.062 nm^{-1}. As mentioned in point number 1, S6 self-assembled very quickly, and its value of q* stayed constant.

3. For the same number of fluorine atoms in the fluorinated block, the BCP having more fluorine in the side chain unit is more likely to microphase separate, and will self-assembly more quickly. BCPs S6 and H4 had the same number of fluorine atoms (7 * 11.1 ≈ 15 * 4.8). Both the q* value and FWHM of BCP H4 changed a little when the annealing condition changed. Additionally, the increase of the chain length of the fluorinated block, going from H2 to H3 to H4 improved the BCP's fast self-assembly behavior. Again, S6 self-assembled very quickly, and its value of q* stayed constant.

From these three comparison experiments, we find that perfluoroalkyl chains played quite an important role in fast self-assembly, and appeared to perform better than heptafluoroalkyl chains. The length of the fluorinated side chain has a significant impact on the phase separation and the kinetics of self-assembly.

References

1   L. Leibler, *Macromolecules,* 1980, **13**, 1602-1617.
2   N. Sakamoto, T. Hashimoto, *Macromolecules,* 1995, **28**, 6825-6834.
3   S. Maheshwari, M. Tsapatsis, F. S. Bates, *Macromolecules,* 2007*, **40***, 6638-6646.